

# THE CANTILEVER STRIP PLATE OF VARYING THICKNESS AND THE CENTRE OF SHEAR

by R. DOUGLAS GREGORY

(Department of Mathematics, University of Manchester, Manchester M13 9PL)

CHARLES C. GU

(Data Analysis Products Division, Mathsoft Inc., Seattle WA 98109, USA)

and FREDERIC Y. M. WAN

(Department of Mathematics, University of California at Irvine, Irvine CA 92697, USA)

[Received 15 May 2000. Revise 16 January 2001]

## Summary

A homogeneous, isotropic plate occupies the region  $0 \leq x_1 \leq \infty$ ,  $|x_2| \leq a$ ,  $|x_3| \leq h$ , where the semi-thickness  $h = h(x_2)$ . The ratio  $h(x_2)/a$  is supposed to be everywhere sufficiently small so that the classical theory of bending of thin plates (of non-uniform thickness) applies. The short end of the plate at  $x_1 = 0$  is clamped while the long sides are free. This cantilever plate is now loaded at  $x_1 = +\infty$  by an applied twisting moment, by a bending moment or by flexure. We solve these problems for the case in which  $h$  varies exponentially with  $x_2$ . We use the projection method which overcomes the difficulty that the boundary conditions lead to severe oscillating singularities in the corners  $(0, \pm a)$ .

Our numerical results show that the values of  $M_{11}$ ,  $V_1$  on  $x_1 = 0$  bear little resemblance to those of the corresponding Saint-Venant 'solutions', which do not fully satisfy the boundary conditions at the clamped end. Indeed, very large values of these resultants are found at points near the 'thick' corner which could affect the integrity of the plate in actual engineering applications. We also determine the values of certain weighted integrals of  $M_{11}$ ,  $V_1$ . These constants determine the effect of the clamping at 'large' distances (greater than  $4a$ , say) from the clamped end.

As a further application, we consider the corresponding plate of finite length  $2L$ . Provided that the aspect ratio  $L/a$  is 2 or more, we give accurate approximate solutions for the torsion and flexure of a finite plate clamped at both ends. The flexure problem for the finite plate enables us to calculate the position of the 'centre of shear' according to Reissner's definition. This has not previously been possible due to the complicated nature of the underlying boundary-value problem. In the limit as  $L/a \rightarrow \infty$ , the shear centre lies at  $x_2 = m_1^B a$ , where  $m_1^B$  is one of the weighted integrals in the *bending* problem.

## 1. Introduction

A *beam* is an elastic body bounded by a cylindrical surface (the lateral surface) and two planes normal to the lateral surface (the end sections). If one end section is fixed, the lateral surface is traction free, and a loading is applied at the other end section, then the beam is said to be

cantilevered. The *shear centre* of a cantilevered beam is conventionally defined as the point in the end section of the beam such that a transverse load applied at that point produces ‘torsionless bending’ of the beam (that is, bending without twisting). However, since the cross-sections of a beam under flexure are all deformed differently, the whole notion of torsionless bending is rather amorphous and different definitions of this concept lead to different positions for the shear centre; see (1, section 53). In addition to this ambiguity, most elementary determinations of the shear centre do not take proper account of the boundary conditions at the ends of the beam. It may be correctly argued that only the resultant forces and moments of the stress distribution at the loaded end are significant away from that end; however, it transpires that the boundary conditions at the fixed end affect the position of the shear centre even in the limit as the length of the beam tends to infinity. Since these displacement boundary conditions make the whole boundary-value problem for the beam difficult to solve, it can be said that there has not yet been a definitive solution of the shear centre problem.

Probably the most satisfactory *formulation* of the shear centre problem is due to Reissner (see (2) and the references therein) where the boundary conditions at *both* ends of the beam may be prescribed in terms of displacements. This formulation results in a clearly defined boundary-value problem in elasticity theory and, since both end sections now suffer only rigid displacements, the requirement that the ‘loaded’ end should undergo torsionless bending is perfectly well defined. The corresponding plate theory formulation of the shear centre problem when the beam is a rectangular plate of non-uniform thickness can be found in (3) and some approximate determinations for the shear centre using this formulation were obtained in (4, 5). However, even for thin plates, there is considerable difficulty in solving the necessary boundary-value problems accurately.

In the present work we use Reissner’s formulation to treat the shear centre problem for the special case in which the cantilever beam is a thin plate whose thickness varies in the chordwise direction. Since the plate is assumed to be symmetrical about its mid-plane, it suffices to determine the chordwise coordinate of the shear centre. The location of the shear centre is found to depend only on the outer asymptotic solution of the boundary-value problem for the cantilevered plate. This outer solution is determined, to within exponentially small terms, by the method of decaying residual states (6). This reduces the problem to the solution of three canonical problems for the corresponding *semi-infinite* cantilevered plate; these canonical problems of torsion, bending and flexure can then be solved by the projection method (7 to 9), which properly takes into account the severe oscillating singularities that occur at the corners of the plate. There are, however, some new complications that did not appear previously: (i) the thickness profile of the plate is not symmetrical about the centreline (otherwise the problem would be trivial) and (ii) the Papkovitch–Fadle (PF) eigenfunctions for a plate strip of non-uniform thickness are much more difficult to obtain than in the uniform thickness case.

The method of solution is illustrated for a plate of exponentially varying thickness profile. Once the three canonical problems have been solved by the projection method, certain weighted integrals of the bending moment and transverse shear resultant at the clamped end can be evaluated. The values of these weighted integrals are all that is needed when the method of decaying residual states is applied to determine the position of the shear centre. Comparisons are made with existing approximate solutions due to Gu and Wan (4). Although none of these approximate methods is capable of predicting the physically important behaviour of the solution near the clamped ends, they do give surprisingly accurate values for the position of the shear centre.

## 2. Description of the canonical problems

### 2.1 General theory of thin plates with varying thickness

Let the region  $\{(x_1, x_2, x_3) : (x_1, x_2) \in \mathcal{A}, |x_3| \leq h\}$ , where  $h = h(x_1, x_2)$ , be occupied by a homogeneous, isotropic, linearly elastic material with Young's modulus  $E$  and Poisson's ratio  $\nu$ . We refer to such a body as a (symmetrical) elastic plate of varying thickness. The symmetry of the plate about the the mid-plane  $x_3 = 0$  means that any small deformation is the sum of a small deformation symmetrical about  $x_3 = 0$  and a second small deformation anti-symmetrical about  $x_3 = 0$ . We are concerned in this paper with small deformations of the second kind. These correspond to 'bending' of the plate (rather than 'stretching') and will ultimately be characterized by  $w(x_1, x_2)$ , the small transverse deflection of the mid-plane  $x_3 = 0$ ; see (10) and the references therein.

The *shear resultants*  $Q_j$  and *moment resultants*  $M_{jk}$  ( $1 \leq j, k \leq 2$ ) are defined in terms of the three-dimensional stress field  $\tau(x_1, x_2, x_3)$  in the plate by

$$Q_j(x_1, x_2) = \int_{-h}^h \tau_{j3}(x_1, x_2, x_3) dx_3 \quad \text{and} \quad M_{jk}(x_1, x_2) = \int_{-h}^h x_3 \tau_{jk}(x_1, x_2, x_3) dx_3.$$

When the faces of the plate on  $x_3 = \pm h$  are free of tractions and body forces are absent, these resultants satisfy the usual equilibrium equations

$$Q_j = M_{1j,1} + M_{2j,2}, \quad (1)$$

$$Q_{1,1} + Q_{2,2} = 0, \quad (2)$$

where  $j = 1, 2$ .

If the plate is 'thin' then the moment resultants  $M_{jk}$  are related to  $w$ , the small transverse deflection of the mid-plane, by the constitutive relations (11)

$$M_{11} = -D(w_{,11} + \nu w_{,22}), \quad M_{22} = -D(w_{,22} + \nu w_{,11}), \quad (3)$$

$$M_{12} = M_{21} = -D(1 - \nu)w_{,12}, \quad (4)$$

where  $D(x_1, x_2)$  is the *local* flexural rigidity, given by

$$D = \frac{2}{3}Eh^3/(1 - \nu^2). \quad (5)$$

These are the same formulae as in the classical theory of thin plates of constant thickness, except that now  $h = h(x_1, x_2)$ . However, the formulae for  $Q_j$  in terms of  $w$  differ from the constant thickness formulae since they now involve the derivatives of  $D$  with respect to  $x_1$  and  $x_2$ .

With our particular application in mind, we now take  $h$  (and therefore  $D$ ) to depend only on the coordinate  $x_2$ . In this case, the  $Q_j$  are given by

$$Q_1 = -D(w_{,111} + \nu w_{,122}) - (1 - \nu)[Dw_{,12}]_{,2}, \quad (6)$$

$$Q_2 = -D(1 - \nu)w_{,112} - [D(w_{,22} + \nu w_{,11})]_{,2}, \quad (7)$$

while the corresponding *effective* transverse shear resultants  $V_j$  are given by

$$V_1 = Q_1 + M_{12,2} = -D(w_{,111} + \nu w_{,122}) - 2(1 - \nu)[Dw_{,12}]_{,2}, \quad (8)$$

$$V_2 = Q_2 + M_{21,1} = -2D(1 - \nu)w_{,112} - [D(w_{,22} + \nu w_{,11})]_{,2}. \quad (9)$$

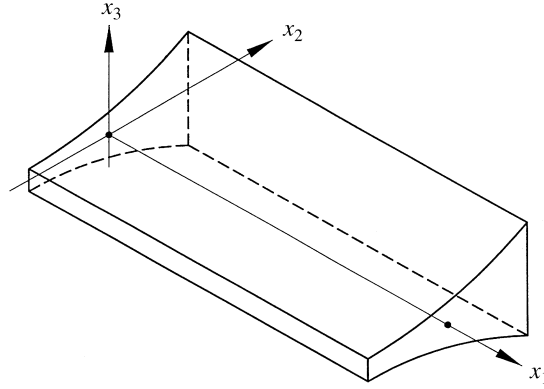


**Fig. 1** The semi-infinite cantilever plate with chordwise varying thickness

On substituting the formulae (6), (7) into the equilibrium equation (2), we obtain the governing equation satisfied by  $w(x_1, x_2)$ , namely

$$D[w_{,1111} + 2w_{,1122} + w_{,2222}] + 2D_{,2}[w_{,222} + w_{,112}] + D_{,22}[w_{,22} + \nu w_{,11}] = 0, \quad (10)$$

for plates whose thickness depends only on the coordinate  $x_2$ .

## 2.2 The cantilever plate with chordwise varying thickness

Consider now the semi-infinite strip plate shown in Fig. 1 which occupies the region  $0 \leq x_1 < \infty$ ,  $|x_2| \leq a$ ,  $|x_3| \leq h(x_2)$ . We suppose that the ratio  $h/a$  is everywhere sufficiently small so that the thin plate theory given above applies. The end of the plate is clamped so that  $w(x_1, x_2)$  satisfies

$$w(0, x_2) = 0, \quad (11)$$

$$w_{,1}(0, x_2) = 0 \quad (12)$$

( $|x_2| \leq a$ ). However the sides of the plate are traction-free so that the Kirchhoff contracted boundary conditions hold, namely

$$M_{22}(x_1, \pm a) = 0, \quad (13)$$

$$V_2(x_1, \pm a) = 0 \quad (14)$$

( $0 < x_1 < \infty$ ). In terms of  $w$ , these boundary conditions take the form

$$w_{,22} + \nu w_{,11} = 0, \quad (15)$$

$$[w_{,22} + (2 - \nu)w_{,11}]_{,2} = 0, \quad (16)$$

after using (15) to simplify (14). The boundary conditions on  $w$  are thus identical to those in the constant thickness case.

This 'cantilever' plate is now loaded at  $x_1 = +\infty$  by one of the following force systems:

- (i) torsion with prescribed twisting moment  $\mathcal{T}$ ,
- (ii) (pure) bending with prescribed bending moment  $\mathcal{M}$ ,
- (iii) flexure with transverse load  $\mathcal{F}$ .

(For the purposes of this paper, it is convenient to use the term ‘flexure’ to mean a combination of transverse load and bending moment so that the applied bending moment at  $x_1 = 0$  is zero. We also suppose that the flexural force has no resultant twisting moment about the axis  $Ox_1$ .)

Some restriction must also be placed on the behaviour of  $w(x_1, x_2)$  near the corner points  $(0, \pm a)$  in order to exclude ‘unphysical’ solutions. We require that the plate should have bounded strain energy near these corners. The precise nature of the corner singularities that are permitted in the constant thickness case has been discussed in (9, Appendix B), and the singularities that occur in the variable thickness case have the same leading terms. These singularities have a profound effect on the solution process.

The problem to be solved in each case is to determine the deflection (and the corresponding shear and moment resultants) in the plate, and especially to determine the unknown resultants  $V_1(0, x_2)$ ,  $M_{11}(0, x_2)$  at the clamped end  $x_1 = 0$ .

### 2.3 The cantilever plate with chordwise exponentially varying thickness

The three problems described above are well-posed boundary-value problems for the transverse displacement  $w(x_1, x_2)$ . However, the governing equation (10) will generally have coefficients that depend on  $x_2$  and this presents analytical difficulty. However, for the case in which  $h(x_2)$  has the exponential form<sup>†</sup>

$$h(x_2) = h_0 e^{2\delta x_2/3a}, \quad (17)$$

where  $h_0, \delta$  are positive constants, the flexural rigidity  $D$  has the exponential form

$$D(x_2) = D_0 e^{2\delta x_2/a}, \quad (18)$$

where  $D_0$  is a positive constant. In this case, the governing equation (10) reduces to

$$[w_{,1111} + 2w_{,1122} + w_{,2222}] + 4\frac{\delta}{a}[w_{,222} + w_{,112}] + 4\left(\frac{\delta}{a}\right)^2 [w_{,22} + \nu w_{,11}] = 0, \quad (19)$$

an equation with *constant coefficients*. This equation is still different from that in the constant thickness case ( $\delta = 0$ ) and has its own difficulties, but these can be overcome.

### 3. The PF-eigenfunctions

From now on we assume that the plate thickness varies exponentially as in (17). Also, we take  $a = 1$  (without losing generality), so that the plate has width 2; the solution for the case of general width can be deduced by scaling.

Our solution method requires the explicit determination of the PF-eigenfunctions for the

<sup>†</sup>The factor 2/3 is introduced for later convenience.

corresponding *infinite* strip problem with the governing equation (19) and the boundary conditions (15), (16) on  $x_2 = \pm 1$ ,  $-\infty < x_1 < \infty$ . These eigenfunctions have the form

$$w^\lambda(x_1, x_2) = e^{-\lambda x_1} E_\lambda(x_2), \quad (20)$$

where the (complex) eigenvalues  $\lambda$  and corresponding functions  $E_\lambda$  are to be determined. The designation PF indicates that these eigenfunctions are analogous to the well-known Papkovitch–Fadle eigenfunctions of plane strain theory. On substituting (20) into equation (19), we find that the function  $E_\lambda$  satisfies

$$E_\lambda'''' + 4\delta E_\lambda''' + (2\lambda^2 + 4\delta^2)E_\lambda'' + 4\delta\lambda^2 E_\lambda' + \lambda^2(\lambda^2 + 4\nu\delta^2)E_\lambda = 0. \quad (21)$$

Although this equation has constant coefficients, its explicit solution would require us to find *analytic* expressions for the roots of a quartic equation whose coefficients depend on the eigenvalue  $\lambda$ . However, if we make the prior change of dependent variable

$$W(x_1, x_2) = e^{\delta x_2} w(x_1, x_2), \quad (22)$$

then  $W$  satisfies

$$W_{,1111} + 2W_{,1122} + W_{,2222} + 2\delta^2(2\nu - 1)W_{,11} - 2\delta^2W_{,22} + \delta^4W = 0 \quad (23)$$

and the boundary conditions on  $x_2 = \pm 1$  become

$$W_{,22} - 2\delta W_{,2} + \delta^2W + \nu W_{,11} = 0, \quad (24)$$

$$W_{,222} - 3\delta W_{,22} + 3\delta^2 W_{,2} - \delta^3 W + (2 - \nu)[W_{,112} - \delta W_{,11}] = 0. \quad (25)$$

The virtue of this transformation is that (23) is now an equation in which odd derivatives are absent. If we now seek the PF-eigenfunctions in the form

$$W(x_1, x_2) = e^{-\lambda x_1} F_\lambda(x_2), \quad (26)$$

then  $F_\lambda$  satisfies

$$F_\lambda'''' + 2(\lambda^2 - \delta^2)F_\lambda'' + [\lambda^4 + 2\delta^2(2\nu - 1)\lambda^2 + \delta^4]F_\lambda = 0 \quad (27)$$

with the boundary conditions

$$F_\lambda'' - 2\delta F_\lambda' + (\delta^2 + \nu\lambda^2)F_\lambda = 0, \quad (28)$$

$$F_\lambda''' - 3\delta F_\lambda'' + (3\delta^2 + (2 - \nu)\lambda^2)F_\lambda' - \delta(\delta^2 + (2 - \nu)\lambda^2)F_\lambda = 0 \quad (29)$$

on  $x_2 = \pm 1$ .

Now equation (27) has solutions of the form

$$F_\lambda = e^{\mu x_2} \quad (30)$$

provided that  $\mu$  satisfies

$$\mu^4 + 2(\lambda^2 - \delta^2)\mu^2 + [\lambda^4 + 2\delta^2(2\nu - 1)\lambda^2 + \delta^4] = 0, \quad (31)$$

which, owing to the transformation (22), is a quadratic equation in the variable  $\mu^2$ . This equation has the solutions

$$\mu^2 = \delta^2 - \lambda^2 \pm 2i\nu^{1/2}\delta\lambda. \quad (32)$$

When the four  $\mu$  values  $\mu_1, \dots, \mu_4$  are distinct, the four functions generated by (30) form a basis set of solutions of the equation (27). Its general solution then has the form

$$F_\lambda(x_2) = c_1 e^{\mu_1 x_2} + c_2 e^{\mu_2 x_2} + c_3 e^{\mu_3 x_2} + c_4 e^{\mu_4 x_2}, \quad (33)$$

where  $c_1, \dots, c_4$  are arbitrary constants. For the sake of definiteness we take

$$\mu_1 = [\delta^2 - \lambda^2 + 2i\nu^{1/2}\delta\lambda]^{1/2}, \quad (34)$$

$$\mu_2 = [\delta^2 - \lambda^2 - 2i\nu^{1/2}\delta\lambda]^{1/2}, \quad (35)$$

$$\mu_3 = -\mu_1, \quad \mu_4 = -\mu_2, \quad (36)$$

where the choice of branches in (34), (35) will turn out to be immaterial.

We now require that the expression (33) satisfy the four boundary conditions (28), (29). (It should be noted that the required solutions have no particular symmetry about the centreline  $x_2 = 0$  so that these four conditions are truly independent.) This leads to a homogeneous system of algebraic linear equations of the form  $\mathbf{A}\mathbf{c} = \mathbf{0}$ , where

$$\mathbf{c} = [c_1, c_2, c_3, c_4]^T \quad (37)$$

and  $\mathbf{A}$  is a  $4 \times 4$  matrix whose elements are known functions of  $\lambda, \delta, \nu$ . A non-trivial solution for  $\mathbf{c}$  will exist if and only if  $\det \mathbf{A} = 0$ . After extensive algebra, this condition reduces to

$$\cosh 2\mu_1 \cosh 2\mu_2 + \frac{\lambda^2 - k\delta^2}{\mu_1 \mu_2} \sinh 2\mu_1 \sinh 2\mu_2 - 1 = 0, \quad (38)$$

where  $\mu_1, \mu_2$  are defined by (34), (35), and  $k = (1 + 14\nu + 17\nu^2)/(1 - \nu)^2$ .

Equation (38) is the eigenvalue equation satisfied by  $\lambda$ . The function on the left is, in fact, an entire function of complex  $\lambda$  and is independent of any choice of branches in the definitions of  $\mu_1, \mu_2$ . It is also an even function of  $\lambda$  and is real when  $\lambda$  is real. The roots must therefore appear in real (or pure imaginary) pairs, or in complex sets of four; ( $\lambda = 0$  is not a root.)

We determined the roots of (38) numerically by starting with the roots for the constant thickness case, corresponding to  $\delta = 0$ . These are the non-zero roots of the equation:

$$\sin^2 2\lambda = \left( \frac{1 - \nu}{3 + \nu} \right)^2 (2\lambda)^2; \quad (39)$$

see (9, Appendix D). The parameter  $\delta$  was assigned a small positive value and the corresponding roots of (38) determined by a complex Newton iteration, using as starting values the roots of (39). The process of incrementing  $\delta$  was successively repeated (at each stage using the previous set of roots as the starting values in a Newton iteration) until the required value of  $\delta$  was attained and the corresponding roots determined. We also determined the asymptotic form of (38) as  $|\lambda| \rightarrow \infty$ , and proved analytically that there must be  $4m - 2$  roots of (38) lying in the complex

domain  $-m\pi/2 < \Re(\lambda) < m\pi/2$  for any sufficiently large integer  $m$ . This was consistent with the number of roots found by our numerical method and confirmed that no roots had been missed.

For each  $\lambda$  satisfying (38), the matrix  $\mathbf{A}$  was found to have rank three. It follows that the corresponding solution vector  $\mathbf{c}^\lambda$  is unique to within normalization and that the eigenfunction corresponding to the eigenvalue  $\lambda$  is given by (20), where

$$E_\lambda(x_2) = e^{-\delta x_2} \sum_{j=1}^4 c_j^\lambda \exp\{\mu_j(\lambda)x_2\}. \quad (40)$$

It remains to dispose of the possibility that the  $\{\mu_j\}$  are not all distinct<sup>‡</sup>. This would occur (i) if  $\mu_1^2 = \mu_2^2$ , or (ii) if either of  $\mu_1, \mu_2$  were zero. In the first case, this would imply that  $\lambda = 0$  which only gives rise to a trivial rigid body deflection. In the second case, suppose that  $\mu_1 = 0$ . This would imply that

$$\lambda = i\nu^{1/2}\delta \pm \delta(1-\nu)^{1/2}. \quad (41)$$

However,  $\lambda$  must also satisfy a determinantal equation similar to (38). We found that the  $\lambda$  values in (41) did not satisfy this second equation.

#### 4. Solution method for the canonical problems

The torsion, bending and flexure problems for the cantilever strip plate with exponentially varying thickness were solved by the ‘method of projection’, which is described in detail in (7,9). We give here a summary of the method. Some new difficulties did arise because the required solutions no longer have any particular symmetry about the centreline  $x_2 = 0$ .

Suppose that  $w(x_1, x_2)$  is the solution for the deflection in (say) the *torsion problem*, with associated moment resultants  $M_{jk}$  and effective shear resultants  $V_j$ . Suppose further that  $w^\lambda, M_{jk}^\lambda, V_j^\lambda$  are the corresponding quantities belonging to the PF-eigenfunction with eigenvalue  $\lambda$ , obtained in section 3. Then it follows from an application of the reciprocity formula obtained in (9, Appendix C), that

$$\int_{-1}^1 [V_1 w^\lambda - M_{11} w_{,1}^\lambda]_{x_1=0} dx_2 = 0, \quad (42)$$

provided that the eigenvalue  $\lambda$  has positive real part (so that  $w^\lambda, M_{jk}^\lambda, V_j^\lambda$  are exponentially *decreasing* as  $x_1 \rightarrow +\infty$ ). This countably infinite set of values of  $\lambda$  will be denoted by  $\Lambda$ . In terms of the function  $E_\lambda$  defined by (39), equation (42) becomes

$$\int_{-1}^1 [V_1(0, x_2)E_\lambda(x_2) + M_{11}(0, x_2)\lambda E_\lambda(x_2)] dx_2 = 0 \quad (43)$$

for all  $\lambda \in \Lambda$ . Formula (43) is a set of identities satisfied by the important unknown resultants  $V_1, M_{11}$  at the clamped end  $x_1 = 0$ .

Gregory and Gladwell (7,8) have devised a method, called the *method of projection*, to determine

<sup>‡</sup>The  $\{\mu_j\}$  are certainly not distinct when Poisson’s ratio  $\nu = 0$ . We exclude this degenerate case from the outset.

the functions  $V_1(0, x_2)$ ,  $M_{11}(0, x_2)$  directly from a system of identities such as (43). Gregory, Gu and Wan (9) improved this method and extended it to accommodate the oscillating singularities present at the corners of a uniform plate with a clamped end and free sides. In the present case, the variable thickness of the plate makes no difference to the *asymptotic* form of the leading Williams eigenfunction (12) in each of the corners. This is because the highest-order terms in the governing equation (19) do not involve  $\delta$  and so are the same as in the uniform plate case. In particular, the leading Williams eigenfunction for the corner at  $(0, 1)$  has resultants on  $x_1 = 0$  of the form

$$V_1(0, x_2) \sim K_1(1 - x_2)^{\alpha+i\beta}, \quad (44)$$

$$M_{11}(0, x_2) \sim K_2(1 - x_2)^{1+\alpha+i\beta} \quad (45)$$

as  $x_2 \rightarrow 1-$ , where  $\alpha$ ,  $\beta$ ,  $K_1/K_2$  depend only on  $\nu$  (the exponents  $\alpha$ ,  $\beta$  are real, but  $K_1/K_2$  is complex in general). Numerical values of  $\alpha$ ,  $\beta$  are given in (9, Appendix B, Table 2) for  $\nu = 1/4, 1/3, 1/2$ . In the torsion problem then, the asymptotic forms of  $V_1(0, x_2)$ ,  $M_{11}(0, x_2)$  as  $x_2 \rightarrow 1-$  must be some (complex) linear combinations of (44), (45) and their complex conjugates.

We now define new unknowns  $\widehat{V}_1(x_2)$ ,  $\widehat{M}_{11}(x_2)$  by

$$V_1(0, x_2) = (1 - x_2^2)^\alpha \widehat{V}_1(x_2), \quad (46)$$

$$M_{11}(0, x_2) = (1 - x_2^2)^{1+\alpha} \widehat{M}_{11}(x_2), \quad (47)$$

in terms of which (43) can be written as

$$\int_{-1}^1 \{(1 - x_2^2)^\alpha \widehat{V}_1(x_2) E_\lambda(x_2) + (1 - x_2^2)^{1+\alpha} \widehat{M}_{11}(x_2) \lambda E_\lambda(x_2)\} dx_2 = 0 \quad (48)$$

for all  $\lambda \in \Lambda$ . When  $\beta = 0$  (which is true when  $\nu$  is very small), the transformation (46), (47) removes the leading term of the corner singularities so that  $\widehat{V}_1$ ,  $\widehat{M}_{11}$  are at least  $C[-1, 1]$ . This greatly simplifies their subsequent determination. For all ‘practical’ values of  $\nu$ , however,  $\beta > 0$  and so  $\widehat{V}_1$ ,  $\widehat{M}_{11}$  still contain part of the corner singularity. They are no longer unbounded, but behave like linear combinations of

$$\cos[\beta \ln(1 - x_2^2)] \quad \text{and} \quad \sin[\beta \ln(1 - x_2^2)] \quad (49)$$

as  $x_2 \rightarrow \pm 1$ , and so have *infinitely many oscillations* of non-vanishing amplitude near  $x_2 = \pm 1$ . This makes their numerical determination very difficult.

In the method of projection the identities (48) are regarded as orthogonality relations. Let  $\mathbf{p}(x_2)$ ,  $\mathbf{q}(x_2)$  be complex-valued two-component vector functions defined almost everywhere on  $[-1, 1]$ . Define the inner-product

$$\langle \mathbf{p}, \mathbf{q} \rangle_\alpha = \int_{-1}^1 \{(1 - x_2^2)^\alpha p_1 \bar{q}_1 + (1 - x_2^2)^{1+\alpha} p_2 \bar{q}_2\} dx_2 \quad (50)$$

with associated norm  $\|\mathbf{p}\|_\alpha = \{\langle \mathbf{p}, \mathbf{p} \rangle_\alpha\}^{1/2}$ . Then  $\mathcal{H}_\alpha \equiv \{\mathbf{p} : \|\mathbf{p}\|_\alpha < \infty\}$  is a Hilbert space under the inner product (50). Since  $\alpha > -1$  in our application, it follows that

$$\widehat{\mathbf{u}} = \begin{pmatrix} \widehat{V}_1 \\ \widehat{M}_{11} \end{pmatrix} \in \mathcal{H}_\alpha, \quad \mathbf{E}_\lambda = \begin{pmatrix} E_\lambda \\ \lambda E_\lambda \end{pmatrix} \in \mathcal{H}_\alpha, \quad (51)$$

and the identities (48) can be written as the orthogonality relations

$$\langle \widehat{\mathbf{u}}, \mathbf{E}_\lambda \rangle_\alpha = 0 \quad (52)$$

for all  $\lambda \in \Lambda$ . In addition to (52),  $\widehat{\mathbf{u}}$  satisfies

$$\left\langle \widehat{\mathbf{u}}, \begin{pmatrix} 0 \\ 1 \end{pmatrix} \right\rangle_\alpha = \left\langle \widehat{\mathbf{u}}, \begin{pmatrix} 1 \\ 0 \end{pmatrix} \right\rangle_\alpha = 0, \quad (53)$$

which implies that there is no applied bending moment or shearing force, and

$$\left\langle \widehat{\mathbf{u}}, \begin{pmatrix} x_2 \\ 0 \end{pmatrix} \right\rangle_\alpha = \mathcal{T}, \quad (54)$$

which implies that the applied twisting moment is  $\mathcal{T}$ .

Let  $\mathcal{D}$  be the linear subspace of  $\mathcal{H}_\alpha$  spanned by

$$\{\mathbf{E}_\lambda\}, \quad \begin{pmatrix} 0 \\ 1 \end{pmatrix}, \quad \begin{pmatrix} 1 \\ 0 \end{pmatrix} \quad (55)$$

( $\lambda \in \Lambda$ ) and let  $\overline{\mathcal{D}}$  be its closure. Then since it may be shown that the orthogonal complement of  $\overline{\mathcal{D}}$  in  $\mathcal{H}_\alpha$  is one-dimensional (see (7)), it follows that  $\widehat{\mathbf{u}}$  is uniquely determined by the orthogonality relations (52), (53) and the normalization equation (54).

The theory developed in (7, 9) now applies to the determination of the unknown vector function  $\widehat{\mathbf{u}}(x_2)$ . In particular, a sequence of approximations convergent to  $\widehat{\mathbf{u}}$  can be constructed as in (7, sections 3, 4), the details of which will not be repeated here. This procedure begins by selecting ‘any’ element  $\mathbf{h}$  of  $\mathcal{H}_\alpha$  not lying in  $\overline{\mathcal{D}}$ . In practice, however, this initial element has to be carefully chosen so as to accelerate the convergence of the approximation process. Essentially  $\mathbf{h}$  is chosen so as to mimic the singular behaviour known to be present in  $\widehat{\mathbf{u}}(x_2)$  at  $x_2 = \pm 1$ ; see (44), (45). This enables  $\mathbf{h} - \widehat{\mathbf{u}}$  to be expanded in a series of smooth functions that converges rapidly. In the uniform thickness case we could exploit the symmetry of the solutions about the centreline  $x_2 = 0$  to simplify the choice of  $\mathbf{h}$ , but in the present case no such symmetry exists and we must allow a correspondingly general  $\mathbf{h}$ .

Consider the ‘singular’ complex vectors  $\mathbf{h}^{\text{SS}}, \mathbf{h}^{\text{SA}}$  given by<sup>§</sup>

$$\mathbf{h}^{\text{SS}} = \begin{pmatrix} 2\frac{K_1}{K_2}(1-x_2^2)^{i\beta} \\ (1-x_2^2)^{i\beta} \end{pmatrix}, \quad \mathbf{h}^{\text{SA}} = \begin{pmatrix} 2\frac{K_1}{K_2}x_2(1-x_2^2)^{i\beta} \\ x_2(1-x_2^2)^{i\beta} \end{pmatrix}, \quad (56)$$

where  $K_1/K_2, \beta$ , which depend only on  $\nu$ , are defined in (44), (45). Then, by a generalization of the argument used in (9, p. 119),  $\mathbf{h}$  is selected from linear combinations of the form

$$\mathbf{h} = a\Re(\mathbf{h}^{\text{SS}}) + b\Im(\mathbf{h}^{\text{SS}}) + c\Re(\mathbf{h}^{\text{SA}}) + d\Im(\mathbf{h}^{\text{SA}}) + e\mathbf{h}^{\text{R}}, \quad (57)$$

where  $a, b, c, d, e$  are constants, and  $\mathbf{h}^{\text{R}}$  is some ‘regular’ element of  $\mathcal{H}_\alpha$  (polynomial in  $x_2$ , for

<sup>§</sup> The factor 2 in the upper components compensates for the fact that the actual behaviour of  $V_1, M_{11}$  near  $x_2 = 1$  involves  $(1-x_2)^\alpha, (1-x_2)^{1+\alpha}$ , whereas, in the definitions (46), (47) we use  $(1-x_2^\alpha), (1-x_2^\alpha)^{1+\alpha}$ .

example). The ‘optimum’ choice of the constants  $a, \dots, e$  is not known beforehand and must be determined as part of the solution process. The normalization equation (54) gives one relation between the constants, but four more are needed. These can be provided by requiring that

$$\widehat{\mathbf{u}} - a\Re(\mathbf{h}^{SS}) - b\Im(\mathbf{h}^{SS}) - c\Re(\mathbf{h}^{SA}) - d\Im(\mathbf{h}^{SA}) = \mathbf{0} \quad (58)$$

at the corner points  $x_2 = \pm 1$ . This is equivalent to the statement that the second Williams eigenfunction in each of the corners  $(0, \pm 1)$  is of order  $o(1)$  as  $x_2 \rightarrow \pm 1$  compared to the leading eigenfunction. We imposed the four conditions (58) on our approximate solution to determine the constants  $a, \dots, e$  approximately. By choosing  $\mathbf{h}$  to be this ‘optimum’ linear combination, we found a remarkable improvement in the speed of convergence of our numerical procedure. This enabled us to determine  $\widehat{\mathbf{u}}$  accurately at low computational cost.

The bending and flexure problems are solved in an almost identical manner. Only (53) and (54) are altered to take account of the different loadings.

## 5. Results for the canonical problems

For the problems under consideration, the corner singularities have a complex exponent (except for very small values of  $\nu$ ). These problems were solved by the projection method described in sections 3, 4 which yields numerical values for  $\widehat{V}_1(x_2)$ ,  $\widehat{M}_{11}(x_2)$ . The physical quantities  $V_1(0, x_2)$ ,  $M_{11}(0, x_2)$  can then be found from (46), (47). Note that, because of the boundary condition (12), the moment resultant  $M_{12}(0, x_2) \equiv 0$ , so that the transverse shear resultant  $Q_1$  and effective transverse shear resultant  $V_1$  are equal at the clamped end  $x_1 = 0$ .

Figures 2 to 4 show graphs of (non-dimensionalized)  $\widehat{V}_1(x_2)$  and  $M_{11}(0, x_2)$  for the three canonical problems of torsion, bending and flexure. (We prefer to show graphs of  $\widehat{V}_1$  rather than  $V_1$  because  $V_1$  is unbounded as  $x_2 \rightarrow \pm a$ .) All these graphs were calculated using  $N = 60$ . We also calculated the numerical values using  $N = 80$ . This made almost no difference to the graphs and suggested that our final values were correct to about three decimal places. Although our graphs do not convey this impression, it is actually true that  $M_{11}(0, \pm a) = 0$  in each case. Likewise the infinitely many undamped oscillations of  $\widehat{V}_1(x_2)$  near  $x_2 = \pm a$  are also invisible. The graphs bear little resemblance to those of  $V_1$  and  $M_{11}$  in the Saint-Venant solutions for the corresponding plate of infinite length. This is because these ‘solutions’ do not include the boundary layer at the clamped end  $x_1 = 0$  and could hardly be expected to represent the true solution there. In particular, all of the (non-zero) Saint-Venant stress resultants have the same sign on whole interval  $-a \leq x_2 \leq a$ , unlike those of the true solutions.

### 5.1 The singularities of $V_1$ at $x_2 = \pm a$

Care should be exercised before attributing direct physical significance to the values of  $V_1(0, x_2)$ ,  $M_{11}(0, x_2)$  near  $x_2 = \pm a$ . The entire solution given here is in the context of the classical theory of thin plates, which is an approximate representation of three-dimensional elasticity, valid when  $h/a$  is small. In particular, it cannot be expected to represent the three-dimensional theory in regions lying within a distance of order  $O(h)$  from a corner. In a more complete theory, the classical solution would be supplemented by ‘corner boundary layers’ with respect to which the classical theory would be the ‘outer’ solution. Nevertheless since

$$V_1(0, x_2) = (1 - x_2^2)^\alpha \widehat{V}_1(x_2), \quad (59)$$

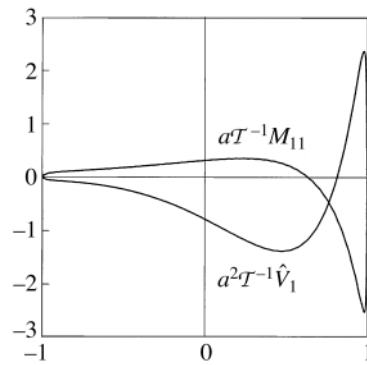


**Fig. 2** Torsion problem: values of  $a^2 T^{-1} \hat{V}_1(x_2)$  and  $a T^{-1} M_{11}(0, x_2)$  against  $x_2/a$  for the plate with thickness profile  $h = h_0 \exp(2x_2/3a)$  and Poisson's ratio  $1/3$

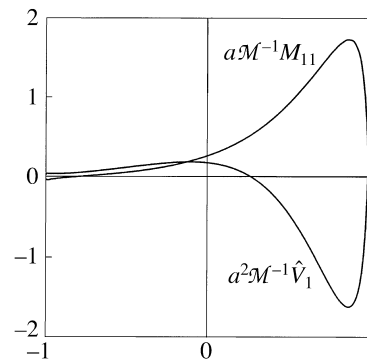


**Fig. 3** Bending problem: values of  $a^2 \mathcal{M}^{-1} \hat{V}_1(x_2)$  and  $a \mathcal{M}^{-1} M_{11}(0, x_2)$  against  $x_2/a$  for the plate with thickness profile  $h = h_0 \exp(2x_2/3a)$  and Poisson's ratio  $1/3$

where the exponent  $\alpha$  is negative, large values of  $V_1$  are actually attainable for physically realistic values of  $h/a$ . Figures 5 to 7 show values of  $V_1(0, x_2)$  for  $x_2$  near  $+a$  (that is, near the 'thick' corner) in the torsion, bending and flexure problems respectively. All these figures show very large values of  $V_1(0, x_2)$  for  $x_2$  near  $a$ . Whether these values are actually attainable depends on the extent of the corner boundary layer which in turn depends on the value of  $h/a$  at the corner. Figure 5 indicates that, in the torsion problem, values of  $V_1$  of about  $18T/a^2$  will be attained provided that the corner boundary layer is negligible at a distance  $a/20$  from the corner; this could certainly happen in engineering applications. The mean value of this quantity in the Saint-Venant torsion 'solution' is  $T/a^2$ . From Figs 6, 7, the corresponding values of  $V_1$  in the bending and flexure problems are about  $10\mathcal{M}/a^2$  and  $5\mathcal{F}/a$  respectively.

The same sort of behaviour is not evident at  $x_2 = -a$ . The reason is that, although the singularity

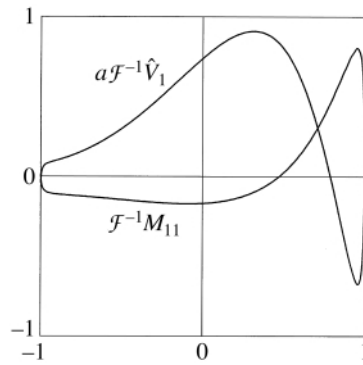


**Fig. 4** Flexure problem: values of  $a\mathcal{F}^{-1}\hat{V}_1(x_2)$  and  $\mathcal{F}^{-1}M_{11}(0, x_2)$  against  $x_2/a$  for the plate with thickness profile  $h = h_0 \exp(2x_2/3a)$  and Poisson's ratio  $1/3$

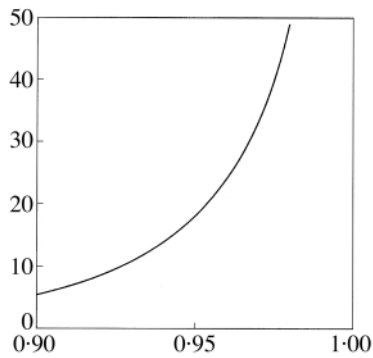


**Fig. 5** Torsion problem: values of  $a^2\mathcal{T}^{-1}V_1(0, x_2)$  for  $x_2$  near  $+a$  for the plate with thickness profile  $h = h_0 \exp(2x_2/3a)$  and Poisson's ratio  $1/3$

at  $x_2 = -a$  is present, it has a very small coefficient because the plate is much thinner there. Thus its numerical effect is much smaller than at the 'thick' corner.

## 5.2 Weighted integrals of $V_1(0, x_2)$ , $M_{11}(0, x_2)$

Of particular importance are certain weighted integrals of  $V_1(0, x_2)$ ,  $M_{11}(0, x_2)$ . These integrals determine the behaviour of the solutions at 'large' distances from the clamped end. They are defined

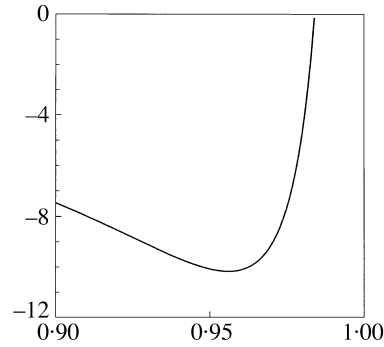


**Fig. 6** Bending problem: values of  $a^2 \mathcal{M}^{-1} V_1(0, x_2)$  for  $x_2$  near  $+a$  for the plate with thickness profile  $h = h_0 \exp(2x_2/3a)$  and Poisson's ratio  $1/3$

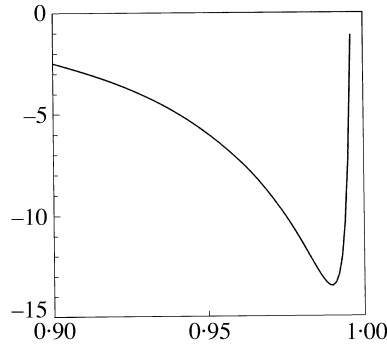


**Fig. 7** Flexure problem: values of  $a \mathcal{F}^{-1} V_1(0, x_2)$  for  $x_2$  near  $+a$  for the plate with thickness profile  $h = h_0 \exp(2x_2/3a)$  and Poisson's ratio  $1/3$

by

$$v_j^T = a^{1-j} \mathcal{T}^{-1} \int_{-a}^a x_2^j V_1^T(0, x_2) dx_2, \quad m_j^T = a^{-j} \mathcal{T}^{-1} \int_{-a}^a x_2^j M_{11}^T(0, x_2) dx_2, \quad (60)$$

$$v_j^B = a^{1-j} \mathcal{M}^{-1} \int_{-a}^a x_2^j V_1^B(0, x_2) dx_2, \quad m_j^B = a^{-j} \mathcal{M}^{-1} \int_{-a}^a x_2^j M_{11}^B(0, x_2) dx_2, \quad (61)$$

$$v_j^F = a^{-j} \mathcal{F}^{-1} \int_{-a}^a x_2^j V_1^F(0, x_2) dx_2, \quad m_j^F = a^{-1-j} \mathcal{F}^{-1} \int_{-a}^a x_2^j M_{11}^F(0, x_2) dx_2, \quad (62)$$

where the suffixes  $T$ ,  $B$ ,  $F$  refer to the torsion, bending and flexure problems respectively, and  $j$  is a positive integer; these quantities are dimensionless and depend only upon  $\nu$  and the plate thickness profile. They are readily calculated once  $V_1(0, x_2)$ ,  $M_{11}(0, x_2)$  have been found, and some of their values are listed in Table 1. As might be expected, these integrated quantities are found more

**Table 1** Values of the constants  $m_1^X, m_2^X, v_2^X$  correct to four decimal places for the plate with thickness profile  $h = h_0 e^{2x_2/3a}$  and Poisson's ratio  $\nu = 1/4, 1/3, 1/2$

	$\nu = 1/4$	$\nu = 1/3$	$\nu = 1/2$
$m_1^T$	-0.3278	-0.3470	-0.3944
$m_2^T$	-0.2206	-0.2344	-0.2688
$v_2^T$	0.9633	0.9655	0.9733
$m_1^B$	0.5596	0.5646	0.5711
$m_2^B$	0.4348	0.4210	0.3825
$v_2^B$	0.3049	0.4030	0.6049
$m_1^F$	0.2025	0.2211	0.2636
$m_2^F$	0.0980	0.0975	0.0963
$v_2^F$	0.1360	0.1889	0.2881

accurately than are the values of the corresponding integrands; with  $N = 80$  they are correct to about six decimal places.

There are valuable checks that can be made on our numerical solutions for the tension, bending and flexure problems. By applying the reciprocity formula in (9, Appendix C) to each pair of solutions, it is readily established that, for any plate thickness profile, the constants  $m_1^T, \dots, v_2^F$  must be related by the three identities

$$m_1^B + \frac{\nu}{1+\nu} v_2^T = K, \quad m_1^F - \frac{\nu}{1+\nu} m_2^T + K m_1^T = 0, \quad (63)$$

$$m_2^B + v_2^F + K v_2^T = \frac{2(1+3\nu) \int_{-a}^a x_2^2 D(x_2) dx_2}{a^2(1+\nu) \int_{-a}^a D(x_2) dx_2}, \quad (64)$$

where

$$K = \frac{(1+3\nu) \int_{-a}^a x_2 D(x_2) dx_2}{a(1+\nu) \int_{-a}^a D(x_2) dx_2}. \quad (65)$$

None of these identities was used in the *calculation* of the solutions, or in the evaluation of the weighted integrals in Table 1, but they were found to be satisfied by our numerical values correct to at least six decimal places.

## 6. Additional deflection as $x_1 \rightarrow \infty$

In each of the torsion, bending and flexure problems, the deflection of the plate as  $x_1 \rightarrow \infty$  approaches that of the corresponding Saint-Venant state, except for an additional rigid body

deflection. This rigid body deflection, which represents the sole effect of the clamped end condition when  $x_1/a$  is large, cannot be found independently and must be determined along with the rest of the solution. To be precise, for *any* plate thickness profile  $h(x_2)$ , the deflection functions  $w^T$ ,  $w^B$ ,  $w^F$  in the torsion, bending and flexure problems have the form

$$w^T(x_1, x_2) = \frac{\mathcal{T}}{4\langle D \rangle(1-\nu)} \left[ \frac{x_1 x_2}{a} + \Theta^T x_2 + \Phi^T x_1 + a W^T \right], \quad (66)$$

$$w^B(x_1, x_2) = \frac{\mathcal{M}}{4\langle D \rangle(1-\nu^2)} \left[ \frac{\nu x_2^2 - x_1^2}{a} + \Theta^B x_2 + \Phi^B x_1 + a W^B \right], \quad (67)$$

$$w^F(x_1, x_2) = \frac{\mathcal{F}a}{12\langle D \rangle(1-\nu^2)} \left[ \frac{3\nu x_1 x_2^2 - x_1^3 - 3Ka(1+\nu)x_1 x_2}{a^2} + \Theta^F x_2 + \Phi^F x_1 + a W^F \right] \quad (68)$$

as  $x_1 \rightarrow \infty$ , with exponentially small error. Here,  $\langle D \rangle$  is the mean flexural rigidity, given by

$$\langle D \rangle = (2a)^{-1} \int_{-a}^a D(x_2) dx_2, \quad (69)$$

and the dimensionless constant  $K$  is defined by (65). The additional rigid body deflections are associated with the dimensionless constants  $\Theta^T$ ,  $\Phi^T$ ,  $\dots$ ,  $W^F$ , which depend only on  $\nu$  and the plate thickness profile. By further applications of the reciprocal formula given in (9, Appendix C), these constants may be expressed in terms of the weighted integrals defined by (60) to (62). After extensive algebra, and use of (63) and (64), the results simplify to

$$\Theta^T = m_1^T, \quad \Phi^T = -m_1^B, \quad W^T = m_1^F, \quad (70)$$

$$\Theta^B = -\nu v_2^T, \quad \Phi^B = \nu v_2^B, \quad W^B = -\nu v_2^F, \quad (71)$$

$$\Theta^F = 3\nu m_2^T - K m_1^T, \quad \Phi^F = -3\nu m_2^B + K m_1^B, \quad W^F = 3\nu m_2^F - K m_1^F. \quad (72)$$

These formulae hold for any plate thickness profile. For the particular case of the exponential profile, some values of the required weighted integrals are given in Table 1.

## 7. Flexure of a plate of finite length and the centre of shear

Let the plate now occupy the region  $|x_1| \leq L$ ,  $|x_2| \leq a$ ,  $|x_3| \leq h(x_2)$  and suppose that its ends at  $x_1 = \pm L$  are held in rigid clamps. Suppose now that the clamps suffer displacements of  $\pm\delta$  in the  $x_3$ -direction (with no rotation) so that the plate is under flexure. What resultant transverse forces  $\pm\mathcal{F}$  and twisting moments  $\pm\mathcal{T}$  must be applied by the clamps? If the plate was of constant thickness, or had a thickness profile  $h(x_2)$  that was an even function of  $x_2$ , these twisting moments would be zero by symmetry. In general, however, they are not zero and this important fact is associated with the notion of 'centre of shear'.

We will treat the finite plate by regarding each of its ends as the end of an appropriate semi-infinite plate. This procedure is not exact since the elastic fields generated from each end will have an effect at the opposite end. However, by examining the numerical value<sup>¶</sup> of the leading PF-eigenvalue

<sup>¶</sup>The figure given refers to the case in which  $h(x_2) = h_0 e^{2x_2/3a}$ . The value of  $\nu$  makes little difference.

obtained in section 3, one may estimate that the relative error induced is about  $(0.025)^{L/a}$ . Thus, even for a square plate with aspect ratio  $L/a = 1$ , the error induced is about 2.5 per cent, and when  $L/a = 2$  the error is about 0.06 per cent.

Since the symmetry of the plate and the end conditions require that  $w(x_1, x_2)$  be an odd function of  $x_1$ , the interior deflection function  $w^I(x_1, x_2)$  (which excludes contributions decaying exponentially from each end) must have the form

$$w^I(x_1, x_2) = A(3vx_1x_2^2 - x_1^3) + Bx_1x_2 + Cx_1. \quad (73)$$

It follows that  $w^+$ , the contribution to  $w$  that decays away exponentially from the end at  $x_1 = -L$ , takes the boundary values

$$w^+(-L, x_2) = A(3vLx_2^2 - L^3) + B(Lx_2) + C(L) - \delta, \quad (74)$$

$$w^+_{,1}(-L, x_2) = -A(3vx_2^2 - 3L^2) - B(x_2) - C. \quad (75)$$

However, if this boundary data is to correspond to an exponentially decaying state then it must satisfy the three necessary conditions

$$\int_{-a}^a [V_1^X(0, x_2)w^+(-L, x_2) - M_{11}(0, x_2)w^+_{,1}(-L, x_2)] dx_2 = 0, \quad (76)$$

where  $V_1^X$ ,  $M_{11}^X$  ( $X = T, B, F$ ) refer to the torsion, bending and flexure problems for the corresponding *semi-infinite* plate; see (42) and (9, Appendix C). On substituting (74), (75) into (76), these equations reduce to

$$\begin{aligned} A'(3vv_2^T + 3vm_2^T\epsilon) + B'(1 + m_1^T\epsilon) &= 0, \\ A'(-3 + 3vv_2^B\epsilon + 3vm_2^B\epsilon^2) + B'(m_1^B\epsilon^2) + C' &= 0, \\ A'(-1 + 3vv_2^F\epsilon^2 + 3vm_2^F\epsilon^3) + B'(m_1^F\epsilon^3) + C' &= 1. \end{aligned} \quad (77)$$

Here  $A'$ ,  $B'$ ,  $C'$  are scaled versions of  $A$ ,  $B$ ,  $C$  defined by  $A = \delta A'/L^3$ ,  $B = a\delta B'/L^3$ ,  $C = \delta C'/L$ , the plate aspect ratio  $\epsilon$  is defined by

$$\epsilon = a/L, \quad (78)$$

and the constants  $m_1^T, \dots, v_2^F$  are the weighted integrals defined by (60) to (62). Equations (77) are sufficient to determine the interior solution  $w^I(x_1, x_2)$  and hence the required resultant transverse force  $\mathcal{F}$  and twisting moment  $\mathcal{T}$ . The individual expressions for  $\mathcal{F}$  and  $\mathcal{T}$  are algebraically complicated but, when expanded in powers of the aspect ratio  $\epsilon (= a/L)$ , we find that  $\mathcal{F}$  is given by

$$\delta = \frac{\mathcal{F}L^3}{12\langle D \rangle(1 - \nu^2)a} [2 - 3vv_2^B\epsilon + 3v(v_2^F - m_2^B + v_2^T m_1^B)\epsilon^2 + O(\epsilon^3)] \quad \text{as } \epsilon \rightarrow 0. \quad (79)$$

The ratio  $\mathcal{T}/\mathcal{F}$  is however given exactly by (77)<sub>1</sub> as

$$\frac{\mathcal{T}}{\mathcal{F}} = Ka - \frac{va}{1 + \nu} \left( \frac{v_2^T + m_2^T\epsilon}{1 + m_1^T\epsilon} \right), \quad (80)$$

where  $K$  is given by (65). On making use of the identities (63) (true for any thickness profile), this can be written simply as

$$\frac{\mathcal{T}}{\mathcal{F}} = \left( \frac{m_1^B - m_1^F\epsilon}{1 + m_1^T\epsilon} \right) a. \quad (81)$$

### 7.1 The centre of shear

The quantity  $\mathcal{T}/\mathcal{F}$  is the  $x_2$ -coordinate of the position of the shear centre of the plate, according to Reissner's definition (3,5). The shear centre, also called the centre of flexure, is sometimes vaguely defined as the point in the end section of a cantilever beam such that a transverse load applied at that point produces 'torsionless bending' (that is, bending without twisting). However, since the cross-sections of a beam under flexure are all differently deformed, the notion of torsionless bending is not actually well defined. Away from the ends of the beam, the elastic field may be approximated by the interior solution, which is a linear combination of the Saint-Venant flexure and torsion solutions for the corresponding infinite beam. As a possible definition of torsionless bending, one could require that (in this interior region) the *mean local twist* over each cross-section should vanish. When restricted to a beam which is a plate of non-uniform thickness, this condition leads to the value  $Y_S^{(1)}$  for the  $x_2$ -coordinate of the shear centre, given by

$$Y_S^{(1)} = \frac{(1+3\nu) \int_{-a}^a x_2 D(x_2) dx_2}{(1+\nu) \int_{-a}^a D(x_2) dx_2} - \frac{2\nu Y_C}{1+\nu}, \quad (82)$$

where  $Y_C$  is the  $x_2$ -coordinate of the centroid of the cross-section. The same value is obtained by imposing the alternative condition that the local twist at the centroid should vanish. On the other hand, if one requires that the shear centre be determined by the condition that the local twist should vanish at *itself*, then the shear centre is located at  $Y_S^{(2)}$ , given by

$$Y_S^{(2)} = \frac{\int_{-a}^a x_2 D(x_2) dx_2}{\int_{-a}^a D(x_2) dx_2}, \quad (83)$$

a position independent of  $\nu$ . Interestingly, the same value is predicted by classical beam theory; see, for example, (4). The values of  $Y_S^{(1)}$ ,  $Y_S^{(2)}$  coincide when  $\nu = 0$  but are obviously different in general, the difference between them rising with  $\nu$ . For a plate with exponentially varying thickness  $h = h_0 e^{2x_2/3a}$ ,  $Y_S^{(1)}$  rises from  $0.54a$  when  $\nu = 0$  to  $0.75a$  when  $\nu = 0.5$  while  $Y_S^{(2)}$  remains at the constant value  $0.54a$ .

Both of the above 'positions' for the shear centre are, however, based upon rather arbitrary criteria and neither is directly related to the solution of any practically important boundary-value problem for the beam. In particular, in neither case are the actual boundary conditions at the fixed end of the beam taken into account. However, Reissner (3,5) has proposed a more rational definition of the shear centre position  $Y_S$ , namely the value of  $\mathcal{T}/\mathcal{F}$  in the flexure problem described at the start of this section. This has the distinct advantage that the meaning of the shear centre is clear and unambiguous; it is the position of the effective resultant force required to displace the clamps in the manner prescribed. On the other hand, its practical determination requires the solution of a difficult boundary-value problem that, until now, could only be treated approximately. However, as a result of our earlier calculation, we find that

$$Y_S = \left( \frac{m_1^B - m_1^F \epsilon}{1 + m_1^T \epsilon} \right) a, \quad (84)$$

where the aspect ratio  $\epsilon = a/L$  and the dimensionless constants  $m_1^T$ ,  $m_1^B$ ,  $m_1^F$  are defined by (60) to (62). In particular, in the important limit as  $L/a \rightarrow \infty$ ,

$$Y_S \rightarrow m_1^B a, \quad (85)$$

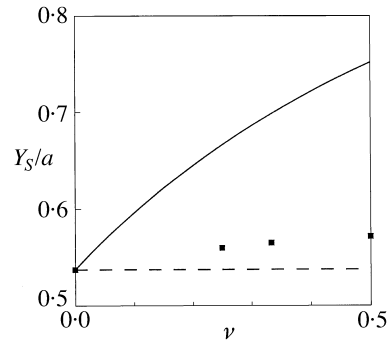


**Fig. 8** The true position of the shear centre  $Y_S$  (squares) compared with  $Y_S^{(1)}$  (solid line) and  $Y_S^{(2)}$  (dashed line) as functions of Poisson's ratio  $\nu$ , for the plate with thickness profile  $h = h_0 e^{2x_2/3a}$

which (curiously) depends only on the solution of the *bending* problem for the semi-infinite plate. Numerical values of  $m_1^B$  for  $\nu = 1/4, 1/3, 1/2$  are given in Table 1.

The value of  $Y_S$  given by (84) is a function of  $a/L$  and  $\nu$  and coincides with the common value of  $Y_S^{(1)}$  and  $Y_S^{(2)}$  when  $\nu = 0$ . However,  $Y_S$  is not strongly dependent on either variable. When  $\nu = 1/2$ , the value of  $Y_S$  when  $a/L = 1$  is about seven per cent less than its value when  $a/L = 0$ . Likewise, when  $a/L = 0$ , the value of  $Y_S$  rises by about six per cent as  $\nu$  increases from 0 to 0.5. Thus, for typical values of  $\nu$ , the true  $Y_S$  happens to be much closer to the constant  $Y_S^{(2)}$  than to the variable  $Y_S^{(1)}$ , which considerably overestimates the true value. This is shown in Fig. 8.

Our exact method can also be used to check on the accuracy of the results of Gu and Wan (4), who determined the shear centre for plates of non-uniform thickness by approximate solutions of the displacement boundary-value problem described in section 7. They used three different approximate methods: generalized beam theory with a quadratic approximation, the same with a cubic approximation, and a finite element method. Since their results refer to a plate with thickness profile  $h = h_0 e^{x_2/a}$  for  $0 \leq x_2 \leq a$ , a separate set of calculations had to be done for the purpose of this comparison. It was found that both of the beam theory results were in error by about one per cent, while the finite element results were accurate to about four decimal places. The success of the finite element method might seem surprising in view of the corner singularities, but Gu and Wan calculated the shear centre from values predicted by the finite element method in the *interior* of the plate, not at the ends. Provided this precaution is taken, the corner singularities clearly do not prevent the finite element method from yielding an accurate value for the shear centre. It should be remembered, however, that none of these approximate methods is effective for calculating the physically important behaviour of the solution at the clamped ends (Figs 2 to 7).

### 8. Torsion of a plate of finite length

In the finite plate problem discussed in the last section, suppose now that the clamped ends at  $x_1 = \pm L$  are rotated through angles  $\pm\alpha$  respectively about the  $x_1$ -axis, so that the plate is under torsion. What resultant twisting moments  $\pm\mathcal{T}$  must be applied to the clamps? Once again the deflection function  $w(x_1, x_2)$  must be an odd function of  $x_1$  and the corresponding interior solution

$w^I(x_1, x_2)$  must have the form (73). The coefficients  $A$ ,  $B$ ,  $C$  are also determined in a similar manner. The complete solution is algebraically complicated but, when expanded in powers of the aspect ratio  $\epsilon$ , we find that  $\mathcal{T}$  is given by

$$\alpha = \frac{\mathcal{T}L}{4(D)(1-\nu)a} \left[ 1 + m_1^T \epsilon + \frac{3\nu}{2} m_1^B v_2^T \epsilon^2 + O(\epsilon^3) \right] \quad (86)$$

as the aspect ratio  $\epsilon \rightarrow 0$ .

Interestingly, the interior solution for the deflection is not  $w^I = \alpha x_1 x_2 / L$ , even at leading order. This is because of a small flexural contribution. The actual formula is

$$w^I(x_1, x_2) = \frac{\alpha x_1}{L} \left[ x_2 + \frac{am_1^B}{2} \left( 1 - \frac{x_1^2}{L^2} \right) + aO(\epsilon) \right] \quad \text{as } \epsilon \rightarrow 0. \quad (87)$$

## References

1. I. S. Sokolnikoff, *Mathematical Theory of Elasticity*, 2nd edn (McGraw–Hill, New York 1956).
2. E. Reissner, Some ramifications of the center of shear problem, *Z. Angew. Math. Mech.* **74** (1992) 315–319.
3. —, The center of shear as a problem of the theory of plates of variable thickness, *Ingenieur-Arch.* **59** (1989) 325–332.
4. C. Gu and F. Y. M. Wan, Approximate solutions for the shear center of plates of variable thickness, *Arch. Appl. Mech.* **63** (1993) 513–521.
5. E. Reissner, Approximate determinations of the center of shear by use of the St Venant solution for the flexure problem of plates of variable thickness, *ibid.* **61** (1991) 555–566.
6. R. D. Gregory and F. Y. M. Wan, Decaying states of plane strain in a semi-infinite strip and the boundary conditions of plate theory, *J. Elast.* **14** (1984) 27–64.
7. — and I. Gladwell, The cantilever beam under tension, bending or flexure at infinity, *ibid.* **12** (1982) 317–343.
8. — and —, The reflection of a symmetric Rayleigh–Lamb wave at the fixed or free edge of a plate, *ibid.* **13** (1983) 185–206.
9. —, C. Gu and F. Y. M. Wan, The cantilever strip plate under torsion, bending or flexure at infinity, *ibid.* **43** (1996) 109–136.
10. —, — and —, Shear center for plates of variable thickness, *Third Asian–Pacific Conference on Computational Mechanics Vol. 1* (ed. C.-K. Choi, C.-B. Yun and D.-G. Lee; Techno-Press, Korea 1996) 299–304.
11. S. Timoshenko and S. Woinowsky-Krieger, *Theory of Plates and Shells*, 2nd edn (McGraw–Hill, New York 1959).
12. M. L. Williams, Surface stress singularities resulting from various boundary conditions in angular corners of plates under bending, *US National Congress of Applied Mechanics* (Illinois Institute of Technology, Chicago, Ill. 1951) 325–329.